Multi-UAS Path-Planning for a Large-scale Disjoint Disaster Management

Younghoon Choi*, Youngjun Choi†, Simon Briceno‡, and Dimitri N. Mavris§

***Abstract*—A UAS-based disaster management method has been adopted to monitor the disaster impact and protect human lives since it can be rapidly deployed, execute an aerial imaging mission, and provide a cost-efficient operation. In the case of a wildfire disaster, a disaster management is highly complex because of large-scale wildfires that can occur simultaneously and disjointly in a large area. In order to effectively manage these large-scale wildfires, it requires multiple UAS with multiple ground stations. However, conventional UAS-based management methods relies on a single ground station that can have a limitation to handle the large-scale wildfire problem. This paper presents a new path-planning framework for UAS operations including a fleet of UAVs and multiple ground stations. The framework consists of two parts: creating coverage paths for each wildfire and optimizing routes for each UAV. To test the developed framework, this paper uses representative wildfire scenarios in the State of California.**

I. Introduction

Recently, unmanned aircraft systems (UAS) have become a promising technology to execute high-risk missions such as monitoring natural disasters and nuclear explosions because of an advanced compact and energy-efficient system. Particularly, the use of UAS is suitable to monitor wildfire that requires fast-response for predicting the future direction of motion of a wildfire and its impact. There are two typical missions for wildfire monitoring: high-altitude disaster monitoring (HADM) and low-altitude fire perimeter monitoring (LAFPM) [1], [2]. The high-altitude disaster monitoring collects comprehensive information in an entire wildfire area to analyze its intensity and damages. The low-altitude fire perimeter monitoring observes the rate of its spread in a real-time manner.

The mission management for both wildfire monitoring missions recently has actively been researched. In the LAFPM mission, Casbeer et al. [3] introduced a decentralized multiple-UAV concept for tracking the propagation of large forest fires that minimizes the information latency and the frequency of update. Phan and Liu [4] proposed the concept of a cooperative forest fire observation with three-layered hierarchical vehicle platforms with a blimp, UAVs, and rovers. For the coordination of the observation task, the paper applies an integer linear programming. Pham et al. [5] suggested the distributed wildfire monitoring management algorithm using a potential field technique for the observation of a dynamic fire trend. Bailon-Ruiz et al. [6] presented the planning algorithm based on a generic variable neighborhood search method to observe spreading wildfires.

The HADM mission is associated with large-scale tasks such as the Western States Fire Mission which provides 24-hour coverage of fires [1], [2]. The HADM mission planning resembles a coverage path planing (CPP) to scan multiple disjoint areas, which builds an optimal coverage route to scan all the disjoint areas [7]. A limitation of these approaches cannot handle large disjoint areas since the optimization framework, a travelling salesman problem (TSP), only considers a single UAV operation. To resolve this limitation, the optimization framework for a multi-UAVs path-planning should be considered to completed the large disjoint areas.

This paper focuses on the HADM problem and introduces a novel multi-UAS path-planning algorithm to monitor multiple and large-scale wildfires. To capture a practical UAS operation, it considers multiple ground stations where UAS are potentially deployed. For the optimal path-planning, we combine an exact CPP method and a multi-depot vehicle routing problem (MDVRP) model that generates computationally efficient monitoring solution through decomposing simpler problems.

This paper is organized as follows: Section II presents the framework for a large-scale wildfire scanning mission with descriptions for each step. Section III shows results of numerical simulations through demonstrating actual wildfire examples occurred in the State of California. This paper ends with conclusions in Section IV.

II. A framework for a UAS-based wildfire scanning mission

Solving VRP is an NP-hard problem that exponentially increases computation time as its problem size increases. In a large-scale wildfire scanning mission, if it has multiple disjoint wildfires with large area, it is easily not solvable because of the complexity. To overcome this computational issue, we proposes a new method that makes more computationally favorable through dividing into two subproblems as shown in Fig. 1: Coverage path-planning and operational planning. The coverage path-planning simply generates actual flight coverage path of each wildfire. The operational planning builds the optimal path that defines the best sequence visiting all the wildfires. This approach can significantly reduce the problem

*Graduate Researcher, School of Aerospace Engineering, Georgia Institute of Technology, younghoon.choi@gatech.edu

†Research Engineer, School of Aerospace Engineering, Georgia Institute of Technology, ychoi95@gatech.edu

‡Senior Research Engineer, School of Aerospace Engineering, Georgia Institute of Technology, briceno@gatech.edu

§S.P. Langley Distinguished Regents Professor, School of Aerospace Engineering, Georgia Institute of Technology, dimitri.mavris@aerospace.gatech.edu

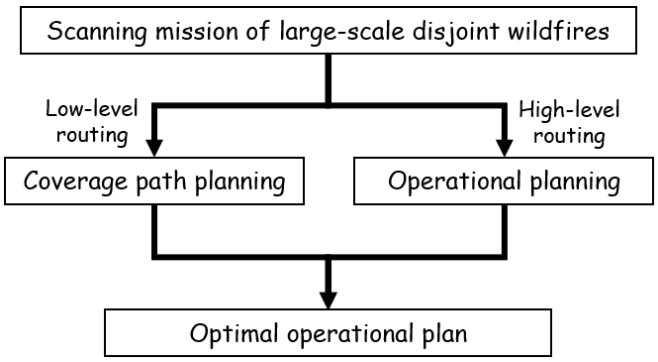

Fig. 1. Notional decomposition of the large-scale scanning mission

size of the optimization model compared to solving the entire problem at once.

A. Coverage path planning for Dubins vehicles

The coverage path planning (CPP) methods for aerial imaging missions have been proposed diverse approaches [8]–[11]. The notable CPP methods can be categorized into three groups: a classical exact method, a wavefront-based method, and a vehicle-routing-based method [11]. The classical exact method creates a Back and Forth Pattern (BFP) path to cover a scanning area, the wavefront-based method applies a wave propagation function that assigns a value of each grid cell and generates a route based on those values. The vehicle-routing-based method formulates an optimization problem that can handle multi-UAV operations to scan a scanning area.

For a HADM mission, high-altitude long-endurance (HALE) UAVs are preferred [2] because typical HADM missions require a long endurance vehicle. This paper assumes that a UAV has a long-endurance platform that can fully observe at least one target area. This assumption allows to create a coverage path of a single UAV for each area by a classical exact method which is faster than other methods because the BFP can be directly utilized without requiring additional computation power to build a trajectory. Thus, this paper utilizes a classical exact method to build a scanning path for each wildfire. The readers interested in the CPP methods may refer the extensive surveys of Galceran and Carreras [12] and Khan et al. [13].

In the CPP problems, minimizing the number of turns is critical to reducing the total mission time or the total energy [14]. The classical exact methods of the CPP decrease the number of turns on their routes by creating the BFP path along the optimal line-sweep direction of the area of interest (AOI). The line-sweep direction of a convex area is determined by a diameter function which is its height in a reference coordinate system calculated by rolling the area. The line-sweep direction having a minimum of the diameter function of a convex area guarantees the minimum number of turns on the BFP route along the direction [14].

As a notional example, let us consider a convex hull modeled by an AOI. When establishing grid cells, a reference

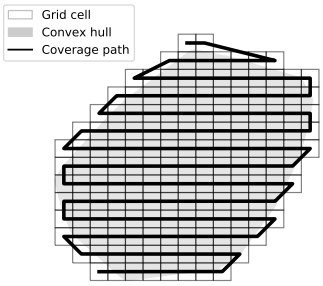

(a) Coverage path without considering a line-sweep direction (26 turns)

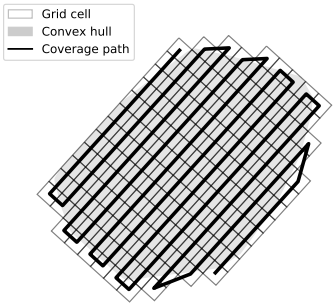

(b) Coverage path along an optimal line-sweep direction (20 turns)

Fig. 2. The effect of a line-sweep direction on creating a coverage path

coordinate system of the whole AOI could be utilized for all target areas. Then, every subarea has the same coordinate system. Figure 2a shows a coverage path built by grid cells defined in a reference coordinate system consisting of a horizontal and a vertical lines. When employing an optimal line-sweep direction for each subarea, a local coordinate system consisting of a line of the direction and a perpendicular line should be created for each subarea. Then, a coverage path built by grid cells defined in the local coordinate system has the number of turns less than or equal to a coverage path in a reference coordinate system as illustrated in Fig. 2b. Note that if a convex hull is not symmetric in terms of its line-sweep direction, the total length of a coverage path depends on its initial scan direction while the paths have the same number of turns. For these cases, we select the shorter path to scan the convex hull created by an AOI.

The BFP path created by classic CPP methods may include sharp turns that occur at a point. To address more realistic turn performance of fixed wing UAVs, the UAVs are considered as Dubins vehicles having a kinematic model as follows:

$$\dot{x} = V\cos\theta \quad (1)$$

$$\dot{y} = V\sin\theta \quad (2)$$

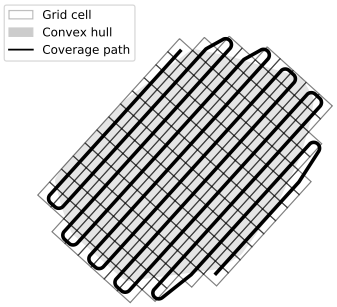

(a) Turns of a Dubins vehicle having enough turning performance

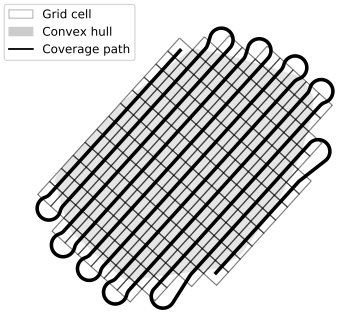

(b) Turns of a Dubins vehicle having not enough turning performance

Fig. 3. The effect of turning performance on turns of a Dubins' vehicle

$$\dot{\theta} \quad = \quad u, \tag{3}$$

where (x, y) is its position, V is the speed, θ is the heading angle, and u is the minimum turning radius or the maximum curvature of the vehicle. Dubins [15] proves that the optimal path between two points constrained by vehicle's heading angle and minimum turning radius has at most CLC or CCC patterns, where C is a turn with its minimum turning radius, and L is a straight line. Johnson [16] and Boissonnat et al. [17] show the same result with control theory.

To address the properties of Dubins vehicles, Dubins paths are built for each pair of two turning points where the scanning direction is changed. The turn performance of UAVs has an effects on a length of curve for turning as illustrated in Fig. 3. If the turn performance of UAVs is not enough to turn between two waypoints, the turn motion requires extra flight time and energy. In this case, reducing the number of turns could be more significant to minimize flight time and energy.

B. Formulations for operational planning

The operational planning is conducted with a simplified flight network that does not consider all the complex low-level flight network. The new network for the operational planning includes two points, mission start/end locations resulting from

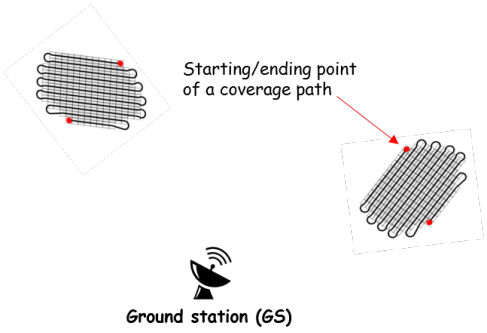

(a) Step 1: finding starting/ending point of each coverage path

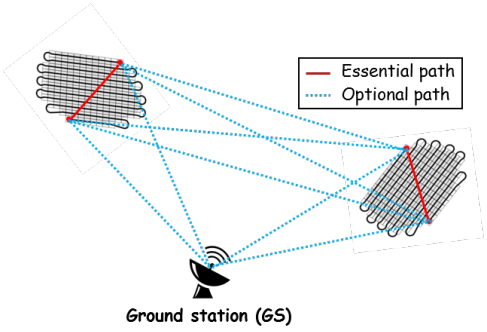

(b) Step 2: creating a flight network as an input of the MDVRP model

Fig. 4. The modeling of mission areas by a graph

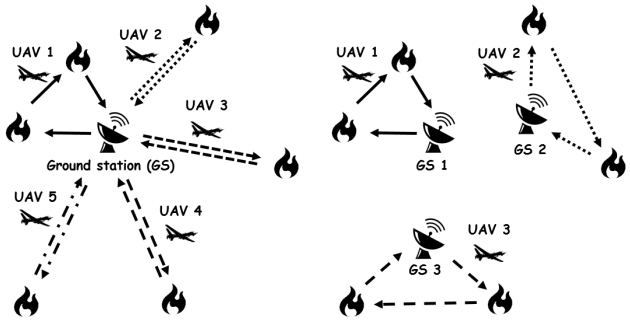

(a) ConOps for the VRP (b) ConOps for the MDVRP

Fig. 5. The effect of vehicle routing formulations on a ConOps

the CPP result, for each target area as shown in Fig. 4a. The new flight network simply connects between a GS and a mission start/end to generate initial potential paths as illustrated in Fig. 4b. In this way, the complexity of initial flight network can significantly reduce; the complexity relies on the topology of the flight network.

The operational planning should consider the concept of operations and the vehicle constraints from UAVs characteristics. To introduce the mathematical formulation of the operational planning, we assume two conceptual examples of a 6-wildfire monitoring mission as shown in Fig. 5: single-GS and multi-GS. In the single-GS scenario with a single UAV, it can be typically modeled by the traveling salesman problem (TSP). In

$$\text{Minimize} \quad \sum_{i\in\mathcal{N}_{NA}}\sum_{j\in\mathcal{N}_{ND}}\sum_{d\in\mathcal{N}_D}\sum_{k\in\mathcal{V}^d}\mathcal{D}_{ij}^{dk}x_{ij}^{dk} \tag{4}$$

Subject to

$$\sum_{j\in\mathcal{N}_{ND}}\sum_{d\in\mathcal{N}_D}\sum_{k\in\mathcal{V}^d}x_{ij}^{dk}=1 \qquad (\forall i\in\mathcal{N}_M) \tag{5}$$

$$\sum_{i\in\mathcal{N}_D}\sum_{j\in\mathcal{N}_{ND}}x_{ij}^{dk}=1 \qquad (\forall d\in\mathcal{N}_D,\forall k\in\mathcal{V}^d) \tag{6}$$

$$\sum_{i\in\mathcal{N}_{NA}}\sum_{j\in\mathcal{N}_A}x_{ij}^{dk}=1 \qquad (\forall d\in\mathcal{N}_D,\forall k\in\mathcal{V}^d) \tag{7}$$

$$\sum_{j\in\mathcal{N}_{ND}}\sum_{k\in\mathcal{V}^d}x_{dj}^{dk}=|\mathcal{V}^d| \qquad (\forall d\in\mathcal{N}_D) \tag{8}$$

$$\sum_{j\in\mathcal{N}_{ND}}x_{dj}^{dk}-\sum_{i\in\mathcal{N}_{NA}}x_{i(d+|D|)}^{dk}=0 \qquad (\forall d\in\mathcal{N}_D,\forall k\in\mathcal{V}^d) \tag{9}$$

$$\sum_{i\in\mathcal{N}_{NA}}x_{ih}^{dk}-\sum_{j\in\mathcal{N}_{ND}}x_{hj}^{dk}=0 \qquad (\forall h\in\mathcal{N}_M,\forall d\in\mathcal{N}_D,\forall k\in\mathcal{V}^d) \tag{10}$$

$$\sum_{d\in\mathcal{N}_D}\sum_{k\in\mathcal{V}^d}x_{ij}^{dk}+\sum_{d\in\mathcal{N}_D}\sum_{k\in\mathcal{V}^d}x_{ji}^{dk}=1 \qquad (\forall(i,j)\in\mathcal{A}_{PM}) \tag{11}$$

$$\sum_{j\in\mathcal{N}_{ND}}y_{ij}^{dk}-\sum_{j\in\mathcal{N}_{NA}}y_{ji}^{dk}-\sum_{j\in\mathcal{N}_{ND}}\mathcal{D}_{ij}^{dk}x_{ij}^{dk}=0 \qquad (\forall i\in\mathcal{N}_M,\forall d\in\mathcal{N}_D,\forall k\in\mathcal{V}^d) \tag{12}$$

$$y_{dj}^{dk}=\mathcal{D}_{dj}^{dk}x_{dj}^{dk} \qquad (\forall j\in\mathcal{N}_{ND},\forall d\in\mathcal{N}_D,\forall k\in\mathcal{V}^d) \tag{13}$$

$$y_{ij}^{dk}\geq(\mathcal{D}_{di}^{dk}+\mathcal{D}_{ij}^{dk})x_{ij}^{dk} \qquad (\forall i\in\mathcal{N}_{NA},\forall j\in\mathcal{N}_{ND},\forall d\in\mathcal{N}_D,\forall k\in\mathcal{V}^d) \tag{14}$$

$$y_{ij}^{dk}\leq(R^{dk}-\mathcal{D}_{j(d+|D|)}^{dk})x_{ij}^{dk} \qquad (\forall i\in\mathcal{N}_{NA},\forall j\in\mathcal{N}_{ND},\forall d\in\mathcal{N}_D,\forall k\in\mathcal{V}^d) \tag{15}$$

$$y_{i(d+|D|)}^{dk}\leq R^{dk}x_{i(d+|D|)}^{dk} \qquad (\forall i\in\mathcal{N}_{NA},\forall d\in\mathcal{N}_D,\forall k\in\mathcal{V}^d). \tag{16}$$

the single-GS scenario with multiple UAVs, a vehicle routing problem (VRP) is typically applied, which is depicted in Fig. 5a. The VRP is a generalized form of the TSP. In the multi-GS scenario with multiple UAVs shown in Fig. 5b, we can implement the multi-depot vehicle routing problem (MDVRP) that optimizes the deployment locations of UAVs and their routes. The MDVRP can have a benefit of having operating cost because UAVs can be deployed the GS closed to the wildfire, and the total mission time and the usage of the number of UAVs can significantly reduce. Because of these benefits, this paper applies the MDVRP to address the wildfire management problem.

To address a generalized delivery system having multiple depots and vehicles, the MDVRP is formulated as a variant of the VRP [18], [19]. In UAS-based applications, the formulations of the MDVRP are used to consider several GSs, which are potential UAV depots, in a post-earthquake assessment mission [20]. The readers interested in the MDVRP could refer the comprehensive survey conducted by Montoya-Torres et al. [21].

To address the MDVRP formulation, we extend the optimization model based on the distance-constrained VRP (DVRP) proposed by Choi et al. [11], which has the generalized formulation of Kara's VRP model [22] to obtain the minimum required number of vehicles. However, this can deal with multiple UASs with a single GS only. The MDVRP as a variant of the VRP considering multiple GSs can be described with graph theory. Mission areas are depicted by a graph, $\mathcal{G}=(\mathcal{N},\mathcal{A})$, and each depot and mission point is modeled by a node. Sets, $\mathcal{N}_D$ and $\mathcal{N}_M$, represent all depots and mission points respectively. In our MDVRP model, an artificial depot node is added for each depot node. A set $\mathcal{N}_A$ indicates all artificial depots. Note that a physical depot is described with two nodes; a depot node and an artificial depot node. The depot node and the artificial depot node are used to represent a starting point and an ending point in a route. For mathematical simplification, we define $|\cdot|$ as the number of elements of a set. For instance, a graph $\mathcal{G}$ includes $|M|$ number of mission points, $M=\{0,1,\cdots,|M|-1\}$, $|D|$ number of depots, $D=\{0,1,\cdots,|D|-1\}$, and $|A|$ number of artificial depots, $A=\{0,1,\cdots,|A|-1\}=\{0,1,\cdots,|D|-1\}$. The set of nodes $\mathcal{N}$ and its subsets are defined such that

$$\begin{aligned}
\mathcal{N}_M &= \{0,1,\cdots,|M|-1\}\\
\mathcal{N}_D &= \{|M|,|M|+1,\cdots,|M|+|D|-1\}\\
\mathcal{N}_A &= \{|M|+|D|,|M|+|D|+1,\cdots,|M|+2|D|-1\}\\
\mathcal{N} &= \mathcal{N}_M\cup\mathcal{N}_D\cup\mathcal{N}_A\\
&= \{0,1,\cdots,|M|+2|D|-1\}=\{0,1,\cdots,|\mathcal{N}|-1\}
\end{aligned}$$

$$\mathcal{N}_{ND} = \mathcal{N} - \mathcal{N}_D = \mathcal{N}_M \cup \mathcal{N}_A$$
$$\mathcal{N}_{NA} = \mathcal{N} - \mathcal{N}_A = \mathcal{N}_M \cup \mathcal{N}_D.$$

An arc presents an edge where a vehicle travels from point A to point B, and the set of arcs $\mathcal{A}$ in the graph $\mathcal{G}$ can be expressed by $\mathcal{A} = \{(i,j) : \forall i \in \mathcal{N}_{NA},\ \forall j \in \mathcal{N}_{ND},\ \text{and } i \neq j\}$. To connect the mission start/end locations in the simplified flight network, a set $\mathcal{A}_{PM} = \{(i, i+1) : \forall i \text{ is an even number of } \mathcal{N}_M\}$ is defined, which corresponds the pair of two locations, mission start/end positions. A set $\mathcal{V} = \bigcup_{d=0}^{|D|-1} \mathcal{V}^d$ indicates a fleet of vehicles and $\mathcal{V}^d$ represents vehicles available at a depot d, $\forall d \in D$, such that $\mathcal{V}^d = \{0, 1, \cdots, |\mathcal{V}^d| - 1\}$, and $\mathcal{V}^{dk}$ is each vehicle at a depot d, $\forall d \in D$, $\forall k \in \mathcal{V}^d$. In the equations, a superscript is related to a depot or a vehicle, and subscripts are associated with an arc. Each vehicle $\mathcal{V}^{dk}$ has its maximum range R^{dk}, where $\forall d \in D$, $\forall k \in \mathcal{V}^d$. The distance from a node i to another node j traveled by a vehicle $\mathcal{V}^{dk}$ is defined as $\mathcal{D}_{ij}^{dk}$ ($\forall (i,j) \in \mathcal{A}$, $\forall d \in D$, $\forall k \in \mathcal{V}^d$). The mathematical formulation has two types of design variables: vehicle movements, x_{ij}^{dk}, and flight distances, y_{ij}^{dk}, where $\forall (i,j) \in \mathcal{A}$, $\forall d \in D$, $\forall k \in \mathcal{V}^d$. This 4-index-based formulation that has been used by Salhi et al. [23] includes starting/ending nodes, originated depots, and a vehicle type. The vehicle movement design variables, x_{ij}^{dk}, are integer variables. The flight distance variables, y_{ij}^{dk}, are real variables having the total flight distance of a vehicle $\mathcal{V}^{dk}$, which flies from a node i to another node j, from a depot d to the node j along its route.

Based on these definitions, an optimization model for multi-depot vehicle routing problems for a UAS-based wildfire monitoring mission in disjoint areas can be written by Eq. (4)-(16). The objective function, Eq. (4), is the total flight distance traveled by all vehicles. The constraints, Eq. (5)-(16), describe the ConOps of a UAS; each mission point is visited by a UAV exactly once, Eq. (5). Each vehicle departs from a depot, Eq. (6), and arrive at a depot, Eq. (7). The number of available vehicles is limited for each depot, Eq. (8). Each vehicle that departs from a depot should return to the same depot, Eq. (9). If a vehicle visits a mission point, it should move to another mission point or a depot, Eq. (10). Eq. (11) presents that the CPP mission should be conducted. When a vehicle moves from a point to another point, its total flight distance increases as much as it flies, Eq. (12), which provides a subtour elimination. The initial flight distance of each vehicle is set by Eq. (13). The lower and upper bounds of flight distance given a vehicle at a specific mission point is written by Eq. (14) and Eq. (15) respectively. The upper bound of flight distance of a vehicle returning to a depot is described by Eq. (16). The overall process of the developed framework for multi-UAS path-planning for a large-scale disjoint disaster management is summarized in Algorithm 1.

Algorithm 1 Framework for multi-UAS path-planning for a large-scale disjoint disaster management

Input: wildfire information, vehicle/GS parameters
Output: optimal routes for each vehicle

PART 1: coverage path planning - [Section II-A]
for each wildfire in wildfires **do**
  Find the convex hull of an area of a wildfire
  Find an optimal line-sweep direction
  Create grid cells based on its local coordinate system
  Build two coverage paths having different scan directions
  Update Dubins paths for each turn
  Select the shorter path
  Extract starting/ending point of the path
end for

PART 2: operational planning - [Section II-B]
Select candidate GSs
Build a flight network based on Dubins paths as an input for the MDVRP model
Solve the MDVRP - [Eq. (4)-(16)]
Combine the solution of the MDVRP model with coverage paths
return Optimal routes for each UAV

III. Numerical simulation

In order to create practical wildfire scenarios, we use historic data of wildfires ignited in the State of California that is obtained on the website of the California Department of Forestry and Fire Protection (CAL FIRE [1]). Furthermore, it is assumed that GSs are general aviation airports in CA, and a UAS platform is the MQ-1 Predator having 1200-km range, and an airborne sensor is modeled based on Zenmuse X5S [10].

This paper addresses three wildfire scanning scenarios. The first scenario describes a path-planning mission to scan a single wildfire with mutiple GSs. The second scenario is designed to compare a single-GS problem and a multi-GS problem to scan multiple wildfires; the GS in a single-GS problem is the closest airport to the centroid of the polygon created from centroids of all wildfires while the GSs in a multi-GS problem are selected by the order of magnitude of the distance from the starting/ending point of each coverage path. The last scenario depicts a large-scale problem consisting of statewide wildfires and GSs. All simulations are executed with Intel® Core™ i7-7700HQ processor and 32-Gb memory. The Gurobi 8.0 is used as a MIP solver to obtain solutions from the optimization models.

The mission of the first scenario is to collect aerial images around the burned area by Thomas Fire, which is fully contained in January 2018. It had affected Ventura and Santa Barbara Counties in CA as shown in Fig. 6. For this aerial imaging mission, it is assumed that four airports are available as shown in Fig. 7. The coverage path planning module initially creates the convex hull of the AOI. Next it builds grid cells in a local reference coordinates presented in Fig. 8, and then creates a scanning trajectory using the BFP. The

[1] http://www.calfire.ca.gov/general/firemaps (accessed 25 January 2019)

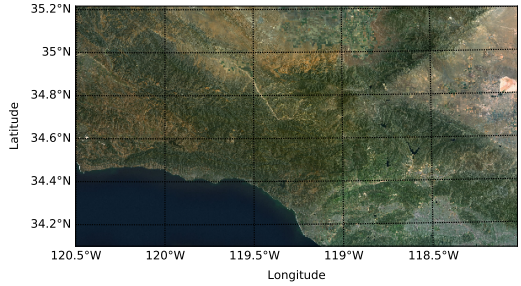

Fig. 6. Area of the January 2018 mission (ArcGIS image)

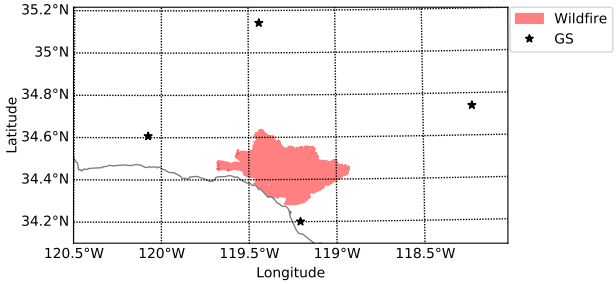

Fig. 7. Thomas Fire fully contained in January 2018 with the nearest GSs

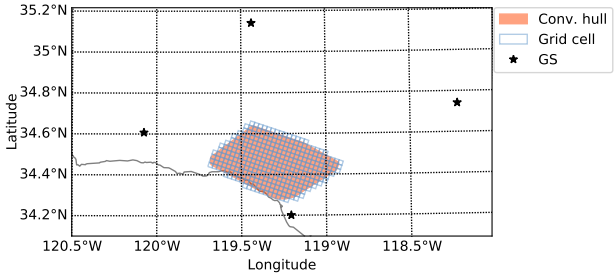

Fig. 8. Grid cells capturing the convex hull of Thomas Fire

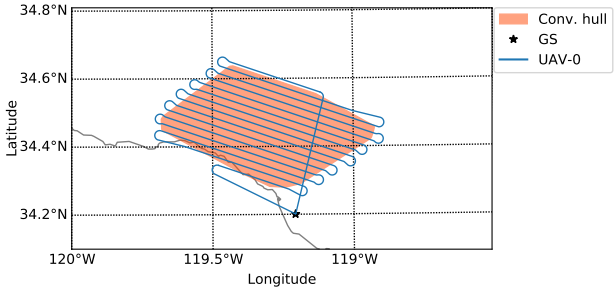

Fig. 9. Route for scanning Thomas Fire

operational planning module solves the MDVRP optimization model based on the CPP result, which selects the optimal GS with an optimal path as visualized in 9. The result is summarized in Table I.

The second scenario has two aerial imaging missions with disjoint multiple wildfires. The first mission is to observe five wildfires, which damaged the areas in southern California in December 2017 as shown in Fig. 10, using a single GS in Fig.

TABLE I
SIMULATION RESULTS OF THOMAS FIRE SCENARIO

Number of fires	Number of req. GSs	Number of req. UAVs	Total flight dist. (km)
1	1	1	957.03

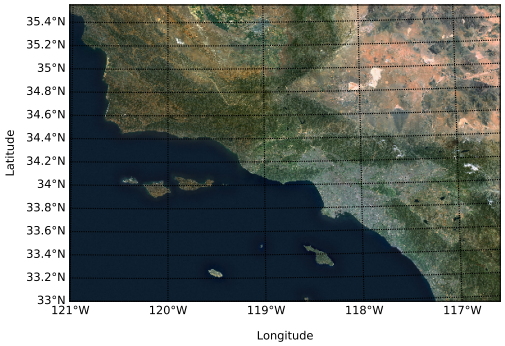

Fig. 10. Area of the December 2017 mission (ArcGIS image)

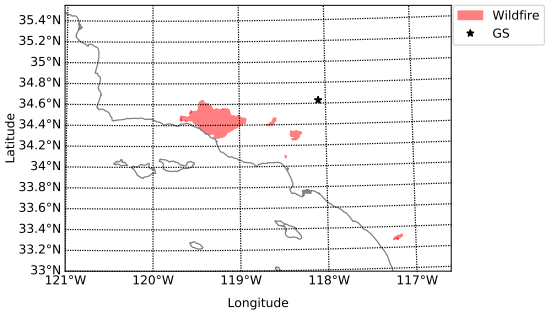

(a) Locations of both wildfires and GS

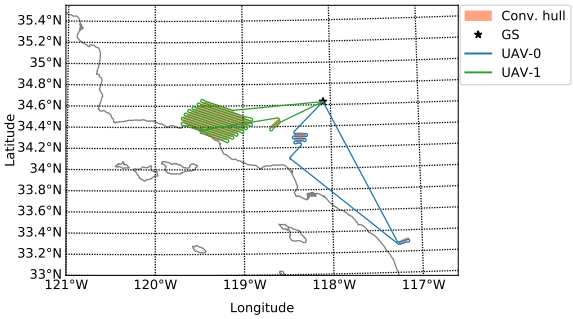

(b) Routes for scanning fires

Fig. 11. Wildfires in December 2017 with a single-GS mission

11a. The result requires two UAVs to scan the entire area of five wildfires as illustrated in Fig 11b. The total flight distance is 1620.99 km. When considering multiple GSs shown in Fig. 12a for the same mission, the improved routes whose the total flight distance is 1224.23 km are created as illustrated in Fig. 12b. These results show that the flight distance is reduced by 24.47 % when multiple GSs are contemplated for the same mission.

The second mission of the second scenario is to look over

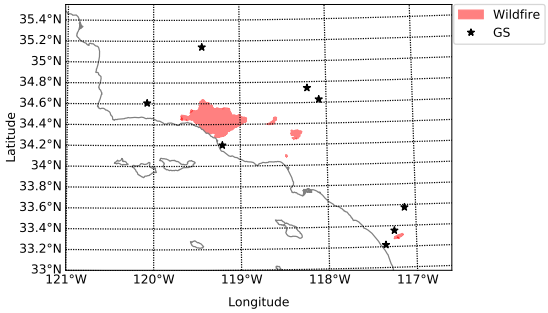

(a) Locations of both wildfires and GSs

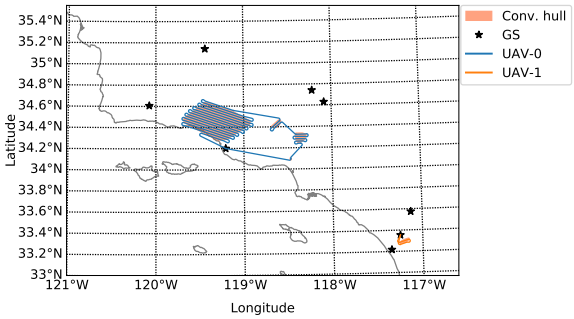

(b) Routes for scanning fires

Fig. 12. Wildfires in December 2017 with a multi-GS scenario

four wildfires which damaged the statewide disjoint area in California in June 2018 as illustrated in Fig. 13. In a single-GS case shown in Fig. 14a, two routes whose the total flight distance is 1926.33 km as depicted in Fig. 14b are created. On the other hand, in a multi-GS case illustrated in Fig.15a, four routes whose the total flight distance is 233.04 km as shown in Fig. 15b, which is reduced by 87.90 % over the single-GS case, are built. These results of two missions show that for operational planning of large-scale disjoint areas, the MDVRP optimization model should be considered to utilize the whole facilities efficiently. The results of the second scenario are summarized in Table II.

The third scenario addresses two statewide fire disasters in both July 2017 and July 2018. The first mission is to sense ten wildfires in July 2017 while the second one is to scan twenty two wildfires in July 2018. These scenarios represent statewide remote sensing missions in fire season in California. The routes of the first mission in Fig. 16 use eight UAVs and GSs while the routes for the second one in Fig. 17 requires sixteen UAVs and GSs to cover all wildfires. The simulation results are shown in Table III. These results show the MDVRP optimization model utilizes the whole facilities to minimize the flight distance which is the objective function of the model. Furthermore, these results implies that the developed framework is applicable to practical problems.

IV. Conclusion

The UAS-based aerial imaging missions have emerged as an essential task to manage a disaster management. This paper introduces a new UAS-based disaster management framework,

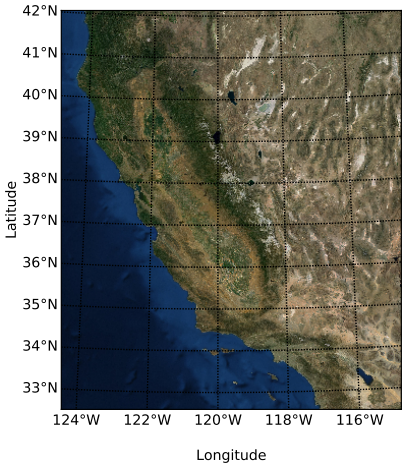

Fig. 13. Map of the statewide California scenarios (ArcGIS image)

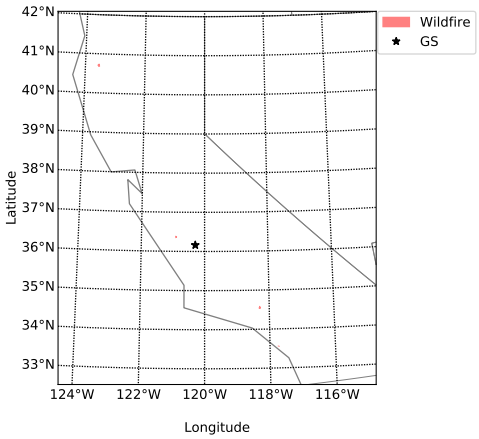

(a) Locations of both wildfires and GS

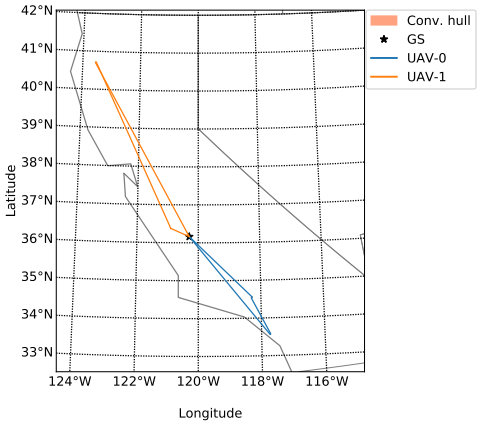

(b) Routes for scanning fires

Fig. 14. Wildfires in June 2018 with a single-GS scenario

particularly for a wildfire mission. The proposed framework can handle large-scale disjoint wildfires efficiently, considering all accessible ground stations. The approach proposed in this paper includes two-level optimal planning: coverage path-planning and operational planing. The coverage path-planning

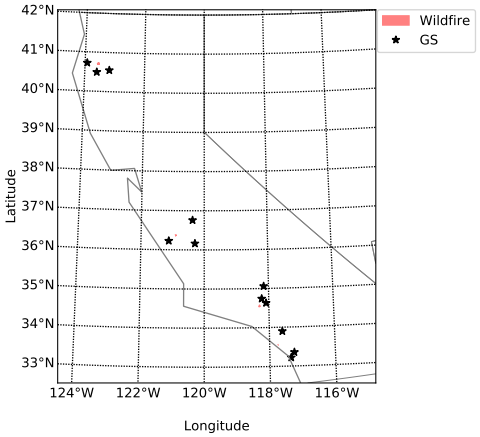

(a) Locations of both wildfires and GSs

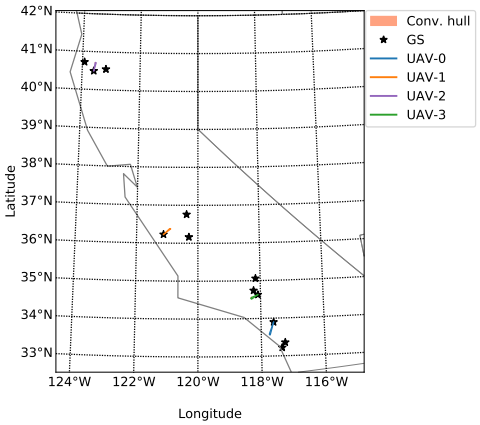

(b) Routes for scanning fires

Fig. 15. Wildfires in June 2018 with a multi-GS scenario

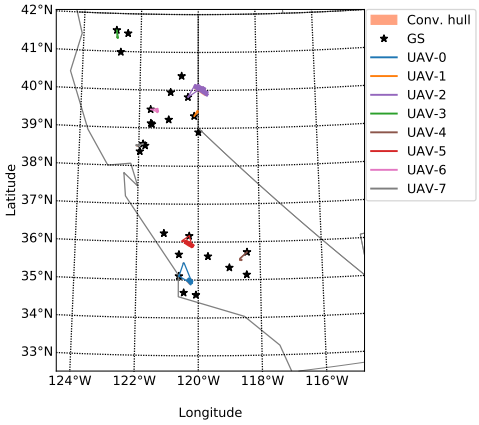

Fig. 16. Routes for sensing wildfires in July 2017

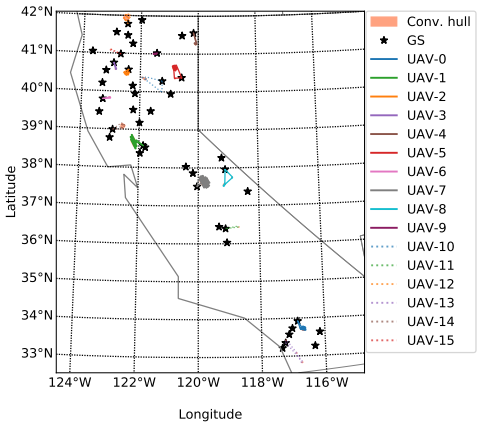

Fig. 17. Routes for sensing wildfires in July 2018

TABLE II
SIMULATION RESULTS OF THE SECOND MISSION

Date	# of fires	GS scen.	# of req. GSs	# of req. UAVs	Total flight dist. (km)
Dec. 2017	5	single	1	2	1620.99
		multiple	2	2	1224.34
June 2018	4	single	1	2	1926.33
		multiple	4	4	233.04

TABLE III
SIMULATION RESULTS OF THE STATEWIDE SCENARIOS

Date	# of fires	# of req. GSs	# of req. UAVs	Total flight dist. (km)
July 2017	10	8	8	1157.71
July 2018	22	16	16	2235.83

provides the low-level path to cover an AOI defined from an wildfire. The operational planing solves MDVRP optimization model to select a UAV deployment location and the sequence of a scanning path. Numerical simulations are conducted to compare with different GS configurations and representative wildfire scenarios using historical data. The results show that the proposed framework provides tangible benefits when multiple GSs are available and multiple disjoint wildfires happen. We believe that the potential extension is including an area decomposition logic either to utilize short-range UAVs or to sense a huge-scale wildfire to make the more computationally efficient algorithm. Considering dynamic wildfire cases also could be a possible extension of this work.

REFERENCES

[1] V. G. Ambrosia, S. S. Wegener, J. A. Brass, and S. M. Schoenung, "The UAV western states fire mission: Concepts, plans and developmental advancements," in *AIAA 3rd "Unmanned Unlimited" Technical Conference, Workshop and Exhibit*, Chicago, IL, September 20-23 2004.

[2] S. S. Wegener, S. M. Schoenung, J. Totah, D. Sullivan, J. Frank, F. Enomoto, C. Frost, and C. Theodore, "UAV autonomous operations for airborne science missions," in *AIAA 3rd "Unmanned Unlimited" Technical Conference, Workshop and Exhibit*, Chicago, IL, September 20-23 2004.

[3] D. W. Casbeer, D. B. Kingston, R. W. Beard, and T. W. McLain, "Cooperative forest fire surveillance using a team of small unmanned air vehicles," *International Journal of Systems Science*, vol. 37, no. 6, pp. 351–360, 2006.

[4] C. Phan and H. H. Liu, "A cooperative UAV/UGV platform for wildfire detection and fighting," in *2008 Asia Simulation Conference - 7th International Conference on System Simulation and Scientific Computing*, Beijing, China, October 10-12 2008.

[5] H. X. Pham, H. M. La, D. Feil-Seifer, and M. Deans, "A distributed control framework for a team of unmanned aerial vehicles for dynamic wildfire tracking," in *IEEE/RSJ International Conference on Intelligent Robots and Systems (IROS)*, Vancouver, BC, Canada, September 24-28 2017.

[6] R. Bailon-Ruiz, A. Bit-Monnot, and S. Lacroix, "Planning to monitor wildfires with a fleet of UAVs," in *2018 IEEE/RSJ International Conference on Intelligent Robots and Systems*, Madrid, Spain, October 2018.

[7] J. I. Vasquez-Gomez, J.-C. Herrera-Lozada, and M. Olguin-Carbajal, "Coverage path planning for surveying disjoint areas," in *The 2018 International Conference on Unmanned Aircraft Systems*, Dallas, TX, June 12-15 2018, pp. 899–904.

[8] C. D. Franco and G. Buttazzo, "Coverage path planning for UAVs photogrammetry with energy and resolution constraints," *Journal of Intelligent and Robotic Systems*, vol. 83, pp. 445–462, 2016.

[9] J. Valente, D. Sanz, J. D. Cerro, A. Barrientos, and M. A. de Frutos, "Near-optimal coverage trajectories for image mosaicing using a mini quad-rotor over irregular-shaped fields," *Precision Agric*, vol. 14, pp. 115–132, 2013.

[10] Y. Choi, Y. Choi, S. Briceno, and D. N. Mavris, "Three-dimensional UAS trajectory optimization for remote sensing in an irregular terrain environment," in *The 2018 International Conference on Unmanned Aircraft Systems*, Dallas, TX, June 12-15 2018, pp. 1101–1108.

[11] Y. Choi, Y. Choi, S. Briceno, and D. N. Mavris, "Coverage path planning for a UAS imagery mission using column generation with a turn penalty," in *The 2018 International Conference on Unmanned Aircraft Systems*, Dallas, TX, June 12-15 2018, pp. 1109–1117.

[12] E. Galceran and M. Carreras, "A survey on coverage path planning for robotics," *Robotics and Autonomous Systems*, vol. 61, pp. 1258–1276, 2013.

[13] A. Khan, I. Noreen, and Z. Habib, "On complete coverage path planning algorithms for non-holonomic mobile robots: survey and challenges," *Journal of Information Science and Engineering*, vol. 33, pp. 101–121, 2017.

[14] W. H. Huang, "Optimal line-sweep-based decompositions for coverage algorithms," in *Proceedings of the 2001 IEEE International Conference on Robotics & Automation*, Seoul, Korea, May 21-26 2001.

[15] L. E. Dubins, "On curves of minimal length with a constraint on average curvature, and with prescribed initial and terminal positions and tangents," *American Journal of Mathematics*, vol. 79, no. 3, pp. 497–516, 1957.

[16] H. H. Johnson, "An application of the maximum principle to the geometry of plane curves," *Proceedings of the American Mathematical Society*, vol. 44, no. 2, pp. 432–435, 1974.

[17] J.-D. Boissonnat, A. Cérézo, and J. Leblond, "Shortest paths of bounded curvature in the plane," *Journal of lntelligent and Robotic Systems*, vol. 11, pp. 5–20, 1994.

[18] B. L. Golden, T. L. Magnanti, and H. Q. Nguyen, "Implementing vehicle routing algorithms," *Networks*, vol. 7, pp. 113–148, 1977.

[19] R. V. Kulkarni and P. R. Bhave, "Integer programming formulations of vehicle routing problems," *European Journal of Operational Research*, vol. 20, pp. 58–67, 1985.

[20] A. Nedjati, G. Izbirak, B. Vizvari, and J. Arkat, "Complete coverage path planning for a multi-UAV response system in post-earthquake assessment," *Robotics*, vol. 26, no. 5, 2016.

[21] J. R. Montoya-Torres, J. L. Franco, S. N. Isaza, H. F. Jimnez, and N. Herazo-Padilla, "A literature review on the vehicle routing problem with multiple depots," *Computers and Industrial Engineering*, vol. 79, pp. 115–129, 2015.

[22] I. Kara, "Arc based integer programming formulations for distance constrained vehicle routing problem," in *LINDI 2011 - 3rd IEEE International Symposium on Logistics and Industrial Informatics*, Budapest, Hungary, August 25-27 2011.

[23] S. Salhi, A. Imran, and N. A. Wassan, "The multi-depot vehicle routing problem with heterogeneous vehicle fleet: Formulation and a variable neighborhood search implementation," *Computers and Operations Research*, vol. 52, pp. 315–325, 2014.